**MATERIAL SCIENCE / МАТЕРИАЛОВЕДЕНИЕ**

**UDC** 669.018.4:621.745.55
**DOI** 10.17073/0368-0797-2023-2-184-190



*Original article*
*Оригинальная статья*

# Influence of laser spot size on structure and properties of high-temperature CompoNiAl-M5-3 alloy produced by selective laser melting

**Yu. Yu. Kaplanskii [1], M. I. Ageev [1], M. Ya. Bychkova [1], A. A. Fadeev [1, 2], E. A. Levashov [1]**

[1] **National University of Science and Technology "MISIS"** (4 Leninskii Ave., Moscow 119049, Russian Federation)
[2] **Baikov Institute of Metallurgy and Materials Science, Russian Academy of Sciences** (49 Leninskii Ave., Moscow 119991, Russian Federation)

ykaplanscky@mail.ru

***Abstract***. The CompoNiAl-M5-3 high-temperature alloy based on nickel monoaluminide was obtained by selective laser melting (SLM) of a spheroidized powder with particle size in the range of 20 – 45 μm. The powder was manufactured using an integral technology including self-propagating high-temperature synthesis (SHS), briquette grinding, sieve and air classification followed with spheroidization of powder particles in a thermal plasma flow and ultrasonic purification of spheroidized particles from nanofraction. Using parametric studies, the SLM modes were tested on SLM 280H and TruPrint 1000 machines. Mechanical tests of the samples were carried out using the uniaxial compression scheme with the strain rate $d\varepsilon/dt = 10^{-4}$ $s^{-1}$ in the temperature range 1023 – 1273 K. Scanning and transmission electron microscopy methods were used to study the influence of laser spot size on the evolution of microstructure and thermomechanical properties of the SLM-consolidated material in comparison with that obtained by hot isostatic pressing (HIP). The authors established the effect of HIP + HT (aging in vacuum) post-treatment on the structure and mechanical properties of the material. The yield strength at 1073 K of the alloy built on the additive machine with a laser spot diameter of 38 μm after SLM + HIP + HT was 500 MPa, which exceeded the yield strength of the HIP-samples by 220 MPa.

***Keywords:*** intermetallic alloys, superalloys, SHS, SHS metallurgy, spherical powders, additive technologies, selective laser melting

***Acknowledgements:*** The study was supported by the Russian Science Foundation, grant No. 19-79-10226, https://rscf.ru/project/19-79-10226/. The authors express their gratitude to Samokhin A.V. and Korotitskii A.V. for their assistance in plasma spheroidization and thermomechanical testing.

***For citation:*** Kaplanskii Yu.Yu., Ageev M.I., Bychkova M.Ya., Fadeev A.A., Levashov E.A. Influence of laser spot size on structure and properties of high-temperature CompoNIAL-M5-3 alloy produced by selective laser melting. *Izvestiya. Ferrous Metallurgy*. 2023;66(2):184–190. *https://doi.org/10.17073/0368-0797-2023-2-184-190*

# Влияние размера пятна лазера на структуру и свойства жаропрочного сплава CompoNiAl-M5-3, полученного селективным лазерным сплавлением

**Ю. Ю. Капланский [1], М. И. Агеев [1], М. Я. Бычкова [1], А. А. Фадеев [1, 2], Е. А. Левашов [1]**

[1] **Национальный исследовательский технологический университет «МИСИС»** (Россия, 119049, Москва, Ленинский пр., 4)
[2] **Институт металлургии и материаловедения им. А.А. Байкова РАН** (Россия, 119991, Москва, Ленинский пр., 49)

ykaplanscky@mail.ru

***Аннотация***. Исследуемый в работе жаропрочный сплав марки CompoNiAl-M5-3 на основе моноалюминида никеля получен методом селективного лазерного сплавления (СЛС) сфероидизированного порошка фракции 20 – 45 мкм. Порошок сплава изготовлен по интегральной технологии, включающей в себя самораспространяющийся высокотемпературный синтез из элементов, измельчение спеков, ситовую и воздушную классификацию, последующую сфероидизацию порошковых частиц в потоке термической плазмы

и ультразвуковую очистку сфероидизированных частиц от нанофракции. Путем параметрических исследований осуществлена отработка режимов СЛС на установках SLM 280H и TruPrint 1000. Механические испытания образцов проведены по схеме одноосного сжатия со скоростью деформирования $d\varepsilon/dt = 10^{-4}$ с$^{-1}$ в интервале температур 1023 – 1273 К. Методами сканирующей и просвечивающей электронной микроскопии исследовано влияние размера пятна лазера на эволюцию микроструктуры и термомеханические свойства консолидированного методом СЛС материала в сравнении с полученным методом горячего изостатического прессования (ГИП). Установлено влияние постобработки ГИП + ТО (старение в вакууме) на структуру и механические свойства материла. Условный предел текучести при 1073 К сплава, выращенного на аддитивной установке с диаметром пятна лазера 38 мкм, в состоянии СЛС + ГИП + ТО составил 500 МПа, что превышает на 220 МПа предел текучести образцов, изготовленных с помощью гранульной металлургии с применением ГИП.

***Ключевые слова:*** интерметаллидные сплавы, жаропрочные сплавы, СВС, СВС-металлургия, сферические порошки, аддитивные технологии, селективное лазерное сплавление

***Благодарности:*** Исследование выполнено за счет гранта Российского научного фонда № 19-79-10226, https://rscf.ru/project/19-79-10226/. Авторы выражают благодарность к.т.н. Самохину А.В. (ИМЕТ РАН) и к.ф.-м.н. Коротицкому А.В. (НИТУ МИСИС) за помощь в проведении плазменной сфероидизации и термомеханических испытаний.

***Для цитирования:*** Капланский Ю.Ю., Агеев М.И., Бычкова М.Я., Фадеев А.А., Левашов Е.А. Влияние размера пятна лазера на структуру и свойства жаропрочного сплава CompoNiAl-M5-3, полученного селективным лазерным сплавлением. *Известия вузов. Черная металлургия*. 2023;66(2):184–190. *https://doi.org/10.17073/0368-0797-2023-2-184-190*

## Introduction

Nickel monoaluminide (NiAl)-based heterophase alloys are utilized as structural material for the production of advanced turbine blades [1 – 3]. These alloys possess several desirable characteristics, including a high congruent melting point of the NiAl matrix (1911 – 1973 K), excellent thermal conductivity ($\lambda \approx 90$ W/(m·K)), relatively low density (<5.5 – 6.8 g/cm$^3$), and superior resistance to oxidation at high-temperatures (>1073 K) compared to nickel superalloys [4 – 6]. However, these alloys exhibit low ductility under normal conditions and are susceptible to microcracking and crack propagation during blade machining and impacts [7 – 9]. These limitations restrict their application for the production ofintricate machined components. An alternative and more promising approach involves additive manufacturing of thin-wall parts (e.g., turbine blade airfoils) without machining processes [10; 11].

Selective laser melting (SLM) offers high precision and excellent surface quality. The quality of thin-walled components relies on the fusion conditions of the walls and the characteristics of equipment, particularly the laser spot size. The laser spot size affects both the surface finish and the metal structure by altering the melt volume during the fusion of the powder layer.

Numerous studies [12 – 16] investigated the compositions and fusion conditions required for manufacturing heat-resistant alloy powders based on NiAl for additive manufacturing purposes. Among these, the structured dispersion-hardened alloy known as CompoNiAl-M5-3 demonstrates the highest mechanical properties at test temperatures up to 1073 K. Additionally, it has been demonstrated that the mechanical properties are influenced by the manufacturing and post-processing technologies, which directly impact the microstructure of the alloy [13; 14]. The cast alloy with a average dendritic cell size of 100 μm and a cluster size of 5 mm exhibits a tensile strength ($\sigma_в$) of up to 1720 MPa and plastic deformation (δ) of up to 8 %. Similarly, an alloy produced through hot isostatic pressing (HIP) of spherical powder in a mold exhibits $\sigma_в = 2870$ MPa (a 40 % increase) and δ = 16.8 %. Furthermore, the alloy demonstrates highly resistant to ductile plastic deformation, with a yield strength ($\sigma_{0.2}$) of up to 392 MPa at 1073 K and a strain rate of 0.01 s$^{-1}$ [14].

According to [14], the significant strength increase in strength can be attributed to the reduction in NiAl grainsize, the presence of coherent solid solution α-Cr precipitations, and dispersed Hf-based particles. Additionally, the formation of thermostable Heisler phase $Ni_2AlHf$ nanoparticles along the grain boundaries contributes to this enhancement. Mechanical properties are further improved by utilizing a fine powder (20 – 45 μm). The powder is produced as follows:

– blending elemental powders;

– self-propagating high-temperature synthesis (SHS);

– grinding the sintered mass into powder;

– air sieve classification;

– plasma spheroidization;

– ultrasonic cleaning of the particles.

The spheroidized powder of the CompoNiAl-M5-3 alloy was successfully employed in the SLM fabrication of power turbine blades [17]. In our study, a similar powder was utilized to investigate the effects of laser spot size on the structure and mechanical properties of the CompoNiAl-M5-3 material.

## Materials and Methods

The spherical powder of the CompoNiAl-M5-3 multicomponent alloy, with a particle size ranging from 20 – 45 μm, was produces through plasma spheroidization of the SHS-powder. The plasma spheroidization was

performed using an arc plasma generator obtained from the Baikov Institute of Metallurgy and Materials Science, Russian Academy of Sciences. The flowability and bulk density of the powder (98 % spheroidization) are 19 s and 3.95 g/cm$^3$, respectively.

For SLM, we employed an industrial-grade SLM 280HL machine (SLM Solution, Germany), equipped with a 400 W fiber laser, and an 80 μm spot size. Additionally, a TruPrint 1000 3D printer (TRUMPF GmbH + Co. KG, Germany) equipped with a 200 W fiber laser and a 38 μm spot size was used. The SLM process parameters were optimized through the fabrication of simple-shape test samples, with variations in the following process variables: laser power $P = 175 \div 330$ W; laser scanning speed $v = 200 \div 500$ mm/s, scanning pitch $h = 0.1 \div 0.12$ mm for SLM 280HL; and $P = 50 \div 90$ W, $v = 400 \div 1000$ mm/s, and $h = 0.05 \div 0.10$ mm for TruPrint 1000.

We assessed the impact of the SLM process conditions on the residual porosity and microcracking. By identifying the optimal SLM condition, we achieved a laser energy density of 120 J/mm$^3$ for SLM 280HL and 97.4 J/mm$^3$ for TruPrint 1000, ensuring that the residual porosity remained below 0.5 %. Subsequently, we fabricated the samples for mechanical testing under these conditions, as depicted Fig. 1.

Heat treatment procedures were previously tested [17]. The samples, together with the build plate, were annealed in a Termionic T1-2000-160 vacuum resistance furnace (Termionic, Russia) at a residual pressure of $1.3 \cdot 10^{-5}$ Pa, with a temperature of 1423 K maintained for 3 h to relieve shrinkage stress. The heat treatment facilitated recrystallization of dendritic cells, grain formation, and dispersion hardening of the matrix by reieasing the excess α-Cr phase [17].

To address micro defects and enhance the mechanical properties of the samples, we employed HIP followed by aging. The samples underwent HIP at 1523 K and 145 MPa, followed by aging in a vacuum at 1073 K for 1.5 h.

The alloy structure was examined using an S-3400N scanning electron microscope (Hitachi, Japan) equipped with a NORAn System 7 X-ray Microanalysis System (Thermo Scientific, USA), and a JEM-2100 high-resolution transmission electron microscope (HP TEM) (Jeol, Japan) equipped with a JEOL Dual Tilt Beryllium Holder. Ultrathin foils for the HP TEM analysis were prepared using a PIPS II ion polishing system (Gatan, Inc., USA).

A uniaxial compression test was conducted using a Gleeble System 3800 thermal and mechanical testing system (Dynamic Systems Inc., USA) to evaluate the material's response to a strain rate of $d\varepsilon/dt = 10^{-4}$ s$^{-1}$ in the temperature range of 1023 – 1273 K. The chamber's residual pressure was approximately $10^{-3}$ Pa.

## Results and Discussion

The microstructure of the samples, shown in Fig. 2 (*XZ* cross-section), revealed the presence of a dendritic grain structure with continuous interlayers of degenerate $Cr(Co)_e$ eutectics (50 – 400 nm thick) in the interdendritic space. Regardless of the fusion conditions of the powder layers, reducing the laser spot size (and laser scanning pitch) from 80 to 38 μm resulted in a halving of the NiAl grains and dendritic cells, accompanied by a decrease in melt volume and solidification time. The cell size decreased from 0.5 – 3.0 μm to 0.2 – 1.0 μm. Hafnium-containing nanoparticles, smaller than 100 nm, were irregularly distributed within the $Cr(Co)_e$ phase or at the NiAl/$Cr(Co)_e$ interface, contributing to dispersion strengthening. The structure and phase composition of the SLM alloy were discussed in [18].

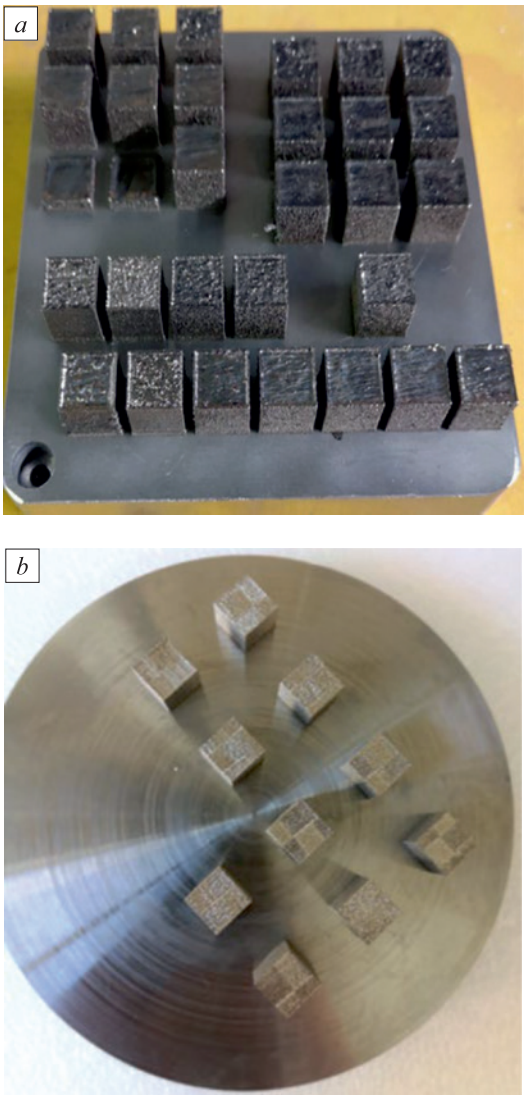


Fig. 1. Samples synthesized on SLM 280HL (*a*) and TruPrint 1000 (*b*) machines

Рис. 1. Внешний вид экспериментальных образцов, синтезированных на установках SLM 280HL (*a*) и TruPrint 1000 (*b*)

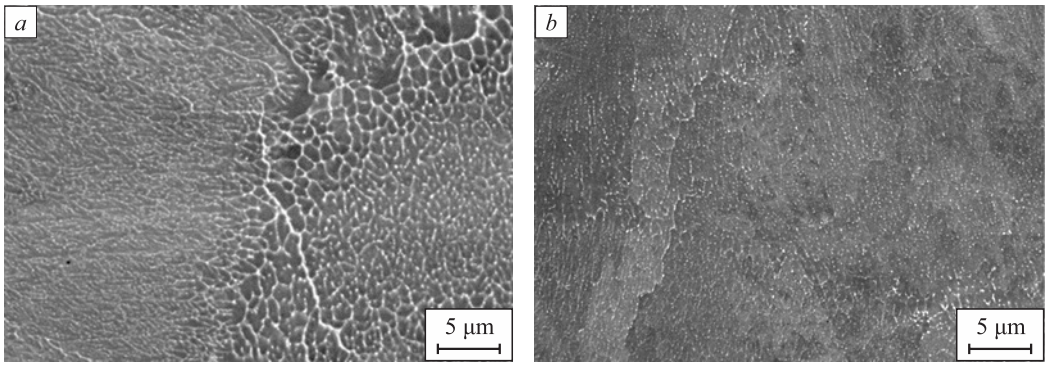


Fig. 2. Microstructure of SLM-samples synthesized on the machines:
*a* – SLM 280HL (laser spot diameter – 80 μm); *b* – TruPrint 1000 (laser spot diameter – 38 μm)

Рис. 2. Микроструктура СЛС-образцов сплава CompoNiAl-M5-3, синтезированных на установках:
*a* – SLM 280HL (диаметр пятна лазера 80 мкм); *b* – TruPrint 1000 (диаметр пятна лазера 38 мкм)

The formation of the dendritic structure can be attributed to the non-equilibrium solidification of the melt during the SLM, occurring at a cooling rate of ~$10^6$ K/s, as well as the presence of excessive chromium content [14; 18].

Fig. 3 illustrates the evolution of the CompoNiAl-M5-3 alloy structure following annealing and gasostatic processing (HT). The annealing process facilitated the recrystallization of NiAl dendritic cells and the formation of uneven grains measured up to 50 μm in size (Fig. 3, *b*, *e*). The alloy structure of the CompoNiAl-M5-3 alloy exhibits α-Cr precipitations, measuring less than 1.5 μm in size, distributed uniformly along the grain boundaries and inside the NiAl grains. These α-Cr precipitations arise from concentration stratification effects within the supersaturated NiAl(Cr) solid solution, occurring both within the grains and at the interfaces of the grain interlayers. Extensive research covered in papers [13; 14; 17; 18] has extensively investigated the mechanisms of α-Cr precipitation growth, including spinodal decay and heterogeneous nucleation, using *in situ* TEM. During the powder bed fusion process, hafnium-containing nanoparticles (indicated by white contrast) precipitate as thin interlayers within the degenerate $Cr(Co)_e$ eutectics. Following annealing, these particles retain their original arrangement and become embedded within the α-Cr precipitation as a result of the $Cr(Co)_e$ segregation.

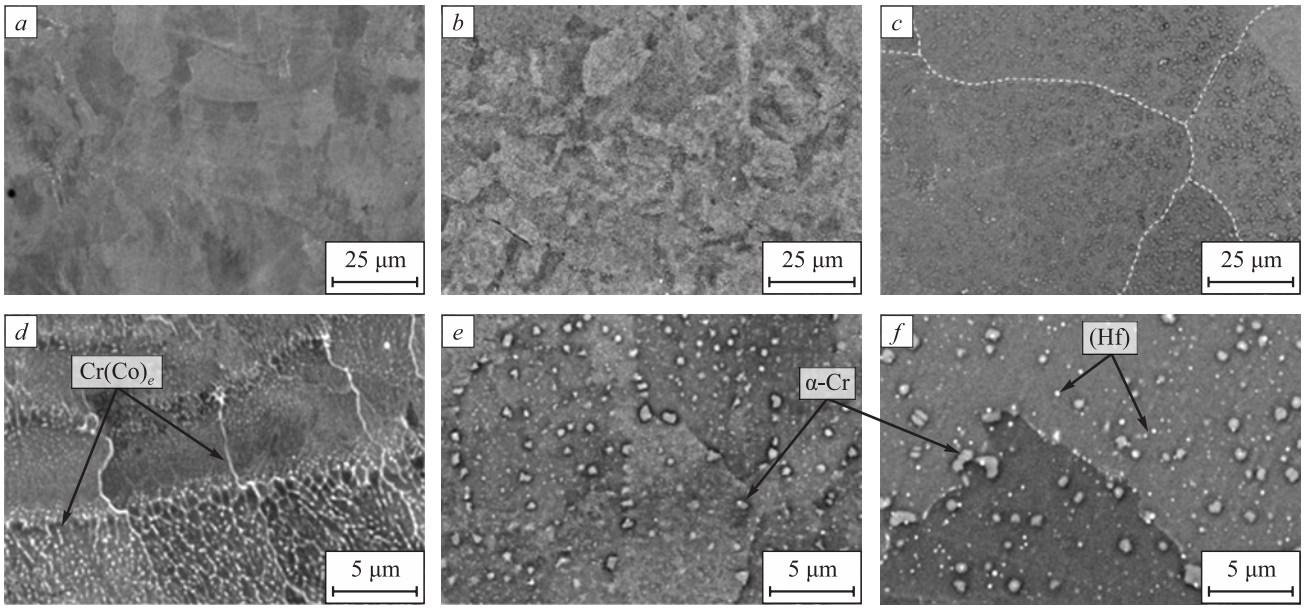


Fig. 3. Structure evolution of CompoNiAl-M5-3 SLM-alloy:
*a*, *d* – initial SLM-samples; *b*, *e* – SLM-samples after annealing; *c*, *f* – annealed SLM-samples after HIP + HT

Рис. 3. Эволюция структуры СЛС-сплава CompoNiAl-M5-3:
*a*, *d* – исходные СЛС-образцы; *b*, *e* – СЛС-образцы после отжига; *c*, *f* – отожженные СЛС-образцы после ГИП + ТО

Through gasostatic processing at 1523 K, the annealed CompoNiAl-M5-3 alloy samples undergo a homogenization process, resulting in a homogeneous, coarse-grained structure composed of the NiAl matrix, α-Cr precipitations, and nanoparticles of the hafnium-containing phases (Fig. 3, *c*, *f*). The grain size ranges from 100 to 450 μm. The significant grain growth observed is attributed to diffusion and threshold creep behavior under simultaneous exposure to high temperature and pressure. At 1523 K, the alloy undergoes a transformation into a single-phase state (supersaturated solid solution). The α-phase is dissolved, and the alloy is homogenized. Upon subsequent cooling within the chamber, α-phase nucleation and growth take place. The excess α-Cr phase precipitations, mainly foung within the grains, exhibit a spherical morphology and reach sizes of up to 1.5 μm. On the contrary, elongated α-Cr particles, measuring up to 3 μm in size, form along the grain boundaries.

Fig. 4 illustrates the yield strength versus temperature curves at a strain rate of $10^{-4}$ $s^{-1}$ for the CompoNiAl-M5-3 alloy samples. The curves compare the samples produced through SLM + HIP + HT using the SLM280HL and TruPrint 1000 machines with samples created through HIP and SLM alone. The resistance to plastic deformation of the SLM samples (SLM280HL) after annealing is comparable to that of the HIP samples when identical spherical powders are used. The two-step post-involving HIP and HT further enhances the compressive stress resistance within the temperature range of 1023 – 1173 K. For example, at 1073 K, the yield strength of the samples after SLM + HIP + HT ranges from 390 to 500 MPa, noticeably higher than the range of 260 – 280 MPa for the SLM and HIP samples. As the temperature increases, the difference diminishes to 11 – 20 MPa. The CompoNiAl-M5-3 alloy samples produsd using the TruPrint 1000 3D printer, with a laser spot size of 38 μm, exhibit the highest resistance throughout the entire temperature range. When comparing samples made through different additive technologies with the same phase compositions, the increase in alloy properties with a decrease in laser spot size and, consequently, the melt volume can be attributed to the refinement and more uniform redistribution of the refractory hafnium-containing phases.

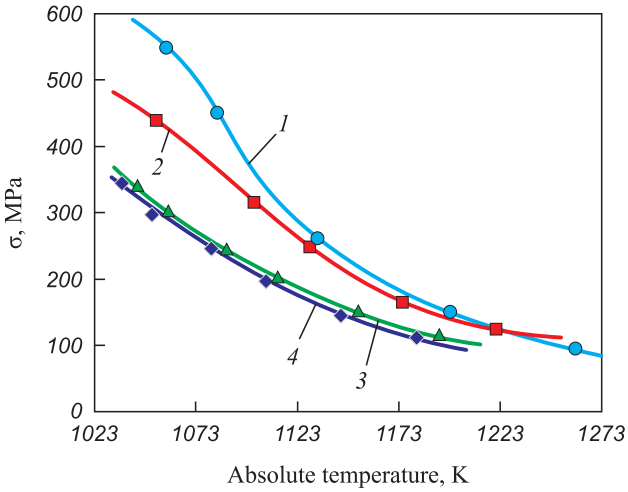


Fig. 4. "Yield strength – temperature" graphs of CompoNiAl-M5-3 samples, obtained by different technologies:
*1* – SLM (TruPrint 1000) + HIP + HT;
*2* – SLM (SLM 280HL) + HIP + HT;
*3* – SLM (SLM280HL); *4* – HIP

Рис. 4. Температурные зависимости условного предела текучести образцов сплава CompoNiAl-M5-3, полученных по различным технологиям:
*1* – СЛС (TruPrint 1000) + ГИП + ТО;
*2* – СЛС (SLM 280HL) + ГИП + ТО;
*3* – СЛС (SLM280HL); *4* – ГИП

The $\sigma_{0.2}$ value at test temperatures up to 1173 K influenced by the alloy structure, particularly the average grain size. The NiAl samples after SLM + HIP + HT exhibit an average grain size of approximately 350 μm, while the HIP and SLM + annealing samples have an average grain size of less than 15 μm. The significant increase in grain size potentially retards Coble creep, as its contribution to the plastic flow becomes more prominent with decreasing temperature and grain size [19 – 22]. Above 1173 K, the alloy's softening rate decreases since the highly coherent α-Cr precipitations within the grain volume, which significantly contribute to alloy hardening within the 1073 K temperature range, dissolve into the matrix.

## Conclusions

The investigation of the microstructure and thermomechanical properties of the CompoNiAl-M5-3 alloy demonstrates that reducing the laser spot size enhances the resistance to ductile plastic deformation at temperatures up to 1173 K. This enhancement is attributed to the grinding process and a more uniform distribution of thermostable hafnium-containing phases within the NiAl matrix.

Gasostatic processing followed by aging in a vacuum further increases the resistance to ductile plastic deformation due to grain coarsening and the hardening effect of coherent precipitations of the excess α-Cr phase.

## References / Список литературы

1. Pelleg J. *Basic Compounds for Superalloys: Mechanical Properties*. Amsterdam: Elsevier Inc.; 2018:494. https://doi.org/10.1016/c2017-0-04724-9
2. Bochenek K., Basista M. Advances in processing of NiAl intermetallic alloys and composites for high temperature aerospace applications. *Progress in Aerospace Sciences*. 2015;79:136–146. https://doi.org/10.1016/j.paerosci.2015.09.003
3. Shang Z., Shen J., Wang L., Du Y., Xiong Y., Fu H. Investigations on the microstructure and room temperature fracture toughness of directionally solidified NiAl–Cr(Mo) eutectic

alloy. *Intermetallics*. 2015;57:25–33. https://doi.org/10.1016/j.intermet.2014.09.012
4. Wu S., Wu X., Wang R., Liu Q., Gan L. Effects of Ni vacancy, Ni antisite, Cr and Pt on the third-order elastic constants and mechanical properties of NiAl. *Intermetallics*. 2014;55: 108–117. https://doi.org/10.1016/j.intermet.2014.04.022
5. Noebe R.D. Physical and mechanical properties of the B2 compound NiAl. *International Materials Reviews*. 2012; 38(4):193–232. https://doi.org/10.1179/imr.1993.38.4.193
6. Wang L., Shen J., Shang Z., Fu H. Microstructure evolution and enhancement of fracture toughness of NiAl–Cr(Mo)–(Hf,Dy) alloy with a small addition of Fe during heat treatment. *Scripta Materialia*. 2014;89:1–4. https://doi.org/10.1016/j.scriptamat.2014.07.002
7. Dey G.K. Physical metallurgy of nickel aluminides. *Sadhana*. 2003;28:247–262. https://doi.org/10.1007/BF02717135
8. Geist D., Gammer C., Rentenberger C., Karnthaler H.P. Sessile dislocations by reactions in NiAl severely deformed at room temperature. *Journal of Alloys and Compounds*. 2015; 621:371–377. https://doi.org/10.1016/j.jallcom.2014.09.226
9. Miracle D.B. Overview No. 104. The physical and mechanical properties of NiAl. *Acta Metallurgica et Materialia*. 1993;41(3):649–684. https://doi.org/10.1016/0956-7151(93)90001-9
10. Gibson I., Rosen D.W., Stucker B. *Additive Manufacturing Technologies: Rapid Prototyping to Direct Digital Manufacturing*. New York: Springer; 2010:459. https://doi.org/10.1007/978-1-4419-1120-9
11. Plessis A. Effects of process parameters on porosity in laser powder bed fusion revealed by X-ray tomography. *Additive Manufacturing*. 2019;30:100871. https://doi.org/10.1016/j.addma.2019.100871
12. Ning H., Wang D., Zhao J., Wang B., Liu G. Fabrication and joining of NiAl and TiAl intermetallics by additive sintering. *Materials Science and Engineering: A*. 2022;849:143493. https://doi.org/10.1016/j.msea.2022.143493
13. Zaitsev A.A., Sentyurina Zh.A., Levashov E.A., Pogozhev Yu.S., Sanin V.N., Loginov P.A., Petrzhik M.I. Structure and properties of NiAl–Cr(Co,Hf) alloys prepared by centrifugal SHS casting. Part 1: Room temperature investigations. *Materials Science and Engineering: A*. 2017;690:463–472. https://doi.org/10.1016/j.msea.2016.09.075
14. Kaplanskii Yu.Yu., Korotitskiy A.V., Levashov E.A., Sentyurina Zh.A., Loginov P.A., Samokhin A.V., Logachev I.A. Microstructure and thermomechanical behavior of Heusler phase $Ni_2AlHf$-strengthened NiAl–Cr(Co) alloy produced by HIP of plasma-spheroidized powder. *Materials Science and Engineering: A*. 2018;729:398–410. https://doi.org/10.1016/j.msea.2018.05.087
15. Nazarov A., Safronov V.A., Khmyrov R.S., Shishkovsky I. Fabrication of gradient structures in the Ni–Al system via SLM Process. *Procedia IUTAM*. 2017;23:161–166. https://doi.org/10.1016/j.piutam.2017.06.017
16. Khomutov M., Potapkin P., Cheverikin V., Petrovskiy P., Travyanov A., Logachev I., Sova A., Smurov I. Effect of hot isostatic pressing on structure and properties of intermetallic NiAl–Cr–Mo alloy produced by selective laser melting. *Intermetallics*. 2020;120:106766. https://doi.org/10.1016/j.intermet.2020.106766
17. Kaplanskii Yu.Yu., Levashov E.A., Korotitskiy A.V., Loginov P.A., Sentyurina Zh.A., Mazalov A.B. Influence of aging and HIP treatment on the structure and properties of NiAl-based turbine blades manufactured by laser powder bed fusion. *Additive Manufacturing*. 2020;31:100999. https://doi.org/10.1016/j.addma.2019.100999
18. Kaplanskii Yu.Yu., Zaitsev A.A., Levashov E.A., Loginov P.A., Sentyurina Zh.A. NiAl based alloy produced by HIP and SLM of pre-alloyed spherical powders. Evolution of the structure and mechanical behavior at high temperatures. *Materials Science and Engineering: A*. 2018;717:48–59. https://doi.org/10.1016/J.MSEA.2018.01.057
19. Kassner M.E. *Fundamentals of Creep in Metals and Alloys*. 3rd Edition. Oxford: Butterworth-Heinemann; 2015:338.
20. *Nanocrystalline Titan*. Garbacz H., Semenova I.P., Zherebtsov S., Motyka M. eds. Amsterdam: Elsevier; 2019:259.
21. Mouritz A.P. *Introduction to Aerospace Materials*. Amsterdam: Elsevier; 2012:600.
22. Zhang J.S. *High Temperature Deformation and Fracture of Materials*. Cambridge: Elsevier; 2010:365.

## Information about the Authors / Сведения об авторах

***Yurii Yu. Kaplanskii,*** *Cand. Sci. (Eng.), Research Associate of the Laboratory "In situ Diagnostics of Structural Transformations" of the Scientific and Educational Center SHS MISiS-ISMAN,* National University of Science and Technology "MISIS"
***ORCID:*** 0000-0002-2153-0743
***E-mail:*** ykaplanscky@mail.ru

***Maksim I. Ageev,*** *Postgraduate of the Chair of Powder Metallurgy and Functional Coatings, Junior Researcher of the Laboratory "In situ Diagnostics of Structural Transformations" of the Scientific and Educational Center SHS MISiS-ISMAN,* National University of Science and Technology "MISIS"
***ORCID:*** 0000-0003-2079-8710
***E-mail:*** aheievmi@gmail.com

***Marina Ya. Bychkova,*** *Cand. Sci. (Eng.), Senior Lecturer of the Chair of Powder Metallurgy and Functional Coatings, Research Associate of the Scientific and Educational Center SHS MISiS-ISMAN,* National University of Science and Technology "MISIS"
***ORCID:*** 0000-0002-9233-4707
***E-mail:*** bychkova@shs.misis.ru

***Юрий Юрьевич Капланский,*** *к.т.н., научный сотрудник лаборатории «In situ диагностика структурных превращений» Научно-учебного центра СВС МИСИС-ИСМАН,* Национальный исследовательский технологический университет «МИСИС»
***ORCID:*** 0000-0002-2153-0743
***E-mail:*** ykaplanscky@mail.ru

***Максим Игоревич Агеев,*** *аспирант кафедры порошковой металлургии и функциональных покрытий, младший научный сотрудник лаборатории «In situ диагностика структурных превращений» Научно-учебного центра СВС МИСИС-ИСМАН,* Национальный исследовательский технологический университет «МИСИС»
***ORCID:*** 0000-0003-2079-8710
***E-mail:*** aheievmi@gmail.com

***Марина Яковлевна Бычкова,*** *к.т.н., старший преподаватель кафедры порошковой металлургии и функциональных покрытий, научный сотрудник Научно-учебного центра СВС МИСИС-ИСМАН,* Национальный исследовательский технологический университет «МИСИС»
***ORCID:*** 0000-0002-9233-4707
***E-mail:*** bychkova@shs.misis.ru

***Andrei A. Fadeev*,** *Cand. Sci. (Eng.), Research Associate,* Baikov Institute of Metallurgy and Materials Science, Russian Academy of Sciences; *Scientific Project Engineer of the Scientific and Educational Center SHS MISiS-ISMAN,* National University of Science and Technology "MISIS"
***ORCID:*** 0000-0003-2147-1787
***E-mail:*** fadeevandrei@gmail.com

***Evgeny A. Levashov*,** *Dr. Sci. (Eng.), Prof., Head of the Chair of Powder Metallurgy and Functional Coatings, Director of the Scientific and Educational Center SHS MISiS-ISMAN,* National University of Science and Technology "MISIS"
***ORCID:*** 0000-0002-0623-0013
***E-mail:*** levashov@shs.misis.ru

***Андрей Андреевич Фадеев*,** *к.т.н., научный сотрудник,* Институт металлургии и материаловедения им. А.А. Байкова РАН; *инженер научного проекта Научно-учебного центра СВС МИСИС-ИСМАН,* Национальный исследовательский технологический университет «МИСИС»
***ORCID:*** 0000-0003-2147-1787
***E-mail:*** fadeevandrei@gmail.com

***Евгений Александрович Левашов*,** *д.т.н., профессор, заведующий кафедрой порошковой металлургии и функциональных покрытий, директор Научно-учебного центра СВС МИСИС-ИСМАН,* Национальный исследовательский технологический университет «МИСИС»
***ORCID:*** 0000-0002-0623-0013
***E-mail:*** levashov@shs.misis.ru

## Contribution of the Authors

***Yu. Yu. Kaplanskii*** – development of SLM modes, microstructural TEM studies, processing and analysis of the experimental results.

***M. I. Ageev*** – synthesis and consolidation of the powder, processing of the experimental results.

***M. Ya. Bychkova*** – microstructural studies, analysis of the experimental results.
***A. A. Fadeev*** – plasma spheroidization of the powder, analysis of the experimental results.
***E. A. Levashov*** – conceptualization of the article, discussion of the results.

## Вклад авторов

***Ю. Ю. Капланский*** – отработка режимов СЛС, проведение микроструктурных исследований методом ПЭМ, обработка и анализ полученных экспериментальных результатов.
***М. И. Агеев*** – проведение работ по синтезу и консолидации порошка сплава, обработка полученных экспериментальных результатов.
***М. Я. Бычкова*** – проведение микроструктурных исследований, анализ полученных экспериментальных результатов.
***А. А. Фадеев*** – проведение работ по плазменной сфероидизации порошка, анализ полученных экспериментальных результатов.
***Е. А. Левашов*** – разработка общей концепции статьи, обсуждение полученных результатов.

Received 07.02.2023
Revised 28.02.2023
Accepted 01.03.2023

Поступила в редакцию 07.02.2023
После доработки 28.02.2023
Принята к публикации 01.03.2023